PNAS RESEARCH ARTICLE | EARTH, ATMOSPHERIC, AND PLANETARY SCIENCES

Narrow range of early habitable Venus scenarios permitted by modeling of oxygen loss and radiogenic argon degassing

Alexandra O. Warren[a,1] and Edwin S. Kite[a]

Edited by Mark Thiemens, University of California, San Diego, La Jolla, CA; received June 11, 2022; accepted January 13, 2023

Whether Venus was ever habitable is a key question driving missions to Earth's sister planet in the next decade. Venus today has a dry, O_2-poor atmosphere, but recent work has proposed that early Venus may have had liquid water [J. Krissansen-Totton, J. J. Fortney, F. Nimmo, *Planet. Sci. J.* 2, 216 (2021)] and reflective clouds that could have sustained habitable conditions until 0.7 Ga [J. Yang, G. Boué, D. C. Fabrycky, D. S. Abbot, *Astrophys. J.* 787, L2 (2014), M. J. Way, A. D. Del Genio, *J. Geophys. Res.: Planets* 125, e2019JE006276 (2020)]. Water present at the end of a habitable era must since have been lost by photodissociation and H escape, causing buildup of atmospheric oxygen [F. Tian, *Earth Planet. Sci. Lett.* 432, 126–132 (2015)]. We present a time-dependent model of Venus's atmospheric composition starting from the end of a hypothetical habitable era with surface liquid water. We find that O_2 loss to space, oxidation of reduced atmospheric species, oxidation of lava, and oxidation of a surface magma layer formed in a runaway greenhouse climate can remove O_2 from up to 500 m global equivalent layer (GEL) (30% of an Earth ocean), unless melts on Venus had a much lower oxygen fugacity than Mid Ocean Ridge melts on Earth, which increases the upper limit twofold. Volcanism is required to supply oxidizable fresh basalt and reduced gases to the atmosphere but also contributes ^{40}Ar. Consistency with Venus's modern atmospheric composition occurs in less than 0.4% of runs, in a narrow parameter range where the reducing power introduced by O_2 loss processes can balance O_2 introduced by H escape. Our models favor hypothetical habitable eras ending before 3 Ga and very reduced melt oxygen fugacities three log units below the fayalite–magnetite–quartz buffer (f_{O_2} < FMQ−3), among other constraints.

Venus | atmospheric evolution | water

Significance

Venus's modern climate is uninhabitable, but early Venus could have sustained surface liquid water for billions of years. Any water present on Venus's surface would have since broken apart into H and O in the atmosphere due to UV radiation, allowing H to escape to space and leaving oxygen behind. Matching Venus's atmospheric composition today after a hypothetical habitable era requires a delicate balance between oxygen sources and loss of oxygen to space and chemical reactions. We find that only a narrow range of conditions enable Venus to have had a habitable era and still evolve to its modern state. Our results suggest that Venus has been uninhabitable for over 70% of its history, four times longer than some previous estimates.

Did Venus ever have liquid water? Answering this question is one of the core questions driving the fleet of new missions to Venus selected by NASA and ESA, the terrestrial planet most similar in size to the Earth in our solar system (1). Today, Venus has an average surface temperature of 720 K, and a dry 93-bar, predominantly CO_2 atmosphere. These conditions preclude the stability of water and most hydrous minerals on its present-day surface (2). Although some studies of Venus's climate evolution suggest that the planet has always been uninhabitably hot (3–5), other modeling studies propose that Venus may have been able to maintain surface temperatures low enough for liquid water for much of its past (6–11). However, a vital question remains: How much water could early Venus have had, and when?

Recent modeling of Venus's magma ocean evolution and subsequent geodynamic and atmospheric evolution suggests that Venus may have retained sufficient water late enough in its history to form an ocean hundreds of meters deep, either through outgassing H_2O from volcanoes or cooling a steam atmosphere (12). Even with modest water inventories of 10 m GEL (Global Equivalent Layer), it has been proposed that habitable conditions on Venus might have persisted until as recently as 0.7 Ga, provided that the planet had a thinner (less than 10-bar) atmosphere, a slow rotation rate, and reflective cloud cover (7, 8).

If a liquid water layer persisted beyond the first few hundred million years of Venus's evolution, it may have left an imprint on Venus's modern atmosphere. This can be used to constrain the maximum thickness of a liquid water layer on Venus. The high deuterium to hydrogen ratio—150 times higher than Earth's (13)—in Venus's atmosphere has been proposed to suggest escape of up to an Earth ocean of water (around 3,000 m GEL) from Venus (14, 15). However, the interpretation of atmospheric D/H remains ambiguous. An Earth ocean of water could have taken anywhere from 4 Gyr to 0.5 Gyr to escape and remain consistent with D/H measurements (16). This range arises from the range of possible hydrogen escape efficiencies and as much as a factor of 20 variability in the D/H fractionation factor over Venus's history (16). Additionally, the water need

Author affiliations: [a]Department of Geophysical Sciences, University of Chicago, Chicago, IL 60637

Author contributions: A.O.W. designed research; A.O.W. performed research; A.O.W. analyzed data; and A.O.W. and E.S.K. wrote the paper.

The authors declare no competing interest.

This article is a PNAS Direct Submission.

Copyright © 2023 the Author(s). Published by PNAS. This article is distributed under Creative Commons Attribution-NonCommercial-NoDerivatives License 4.0 (CC BY-NC-ND).

[1]To whom correspondence may be addressed. Email: aowarren@uchicago.edu.

This article contains supporting information online at http://www.pnas.org/lookup/suppl/doi:10.1073/pnas.2209751120/-/DCSupplemental.

Published March 6, 2023.

Downloaded from https://www.pnas.org by UNIVERSITY OF CHICAGO THE JOHN CRERAR LIBRARY on March 8, 2023 from IP address 128.135.55.25.

not be sourced from an early ocean on Venus. A similar D/H ratio can be produced both by steady-state loss of water delivered over time, for example, by degassing from a fractionated mantle source, through Raleigh fractionation of catastrophic recent water degassing, or through loss of water delivered by impacts (17, 18). Additionally, the initial D/H ratio of Venus may have been higher than for Earth and Mars as a result of its impact history (19) or been modified by loss of H prior to condensation of water on Venus's surface during an early magma ocean period (20). Therefore, although D/H is a useful constraint on the total loss of water from Venus, it is difficult to unpick the effects of Venus's formation and earliest evolution from later H_2O losses from a hypothetical habitable era with surface liquid water.

Fortunately, Venus's atmosphere also records the history of water on the planet through the concentration of atmospheric O (12, 21). Any water in Venus's upper atmosphere is vulnerable to photodissociation to H and O (22). H escapes to space at a higher rate than O, leading to accumulation of O (23). O can then be lost through later nonthermal escape (15, 21), oxidation of reduced atmospheric species such as CO and CH_4 released by volcanoes, and by oxidation of surface rocks (24). Crucial constraints are that Venus's present-day atmosphere is exceedingly O_2 and CO-poor (<70 ppm O_2, <50 ppm CO) and dry (<100 ppm H_2O) (25, 26). Therefore, if Venus ever had oceans, the O added to the atmosphere by the subsequent evaporation of this water during a moist or runaway greenhouse (RGH) period must since have been removed by oxygen sinks (12, 21). In principle, this places an upper limit on the surface water inventory of any habitable period on Venus—i.e., whether or not Venus once had oceans—and also constrains the timing of any possible habitable periods in order to allow time for O sinks to remove essentially all of the O.

Here, we present a time-dependent, mass-balance model of the evolution of Venus's atmospheric composition starting from the end of a hypothetical "habitable era," which we define here as a period able to maintain surface liquid water (Fig. 1; *Materials and Methods*). Previous work has considered Venus's overall evolution from an initial magma ocean phase to explore whether condensation of surface liquid water and consistency with Venus's modern atmosphere are possible (12), but our approach specifically focuses on the consequences of a hypothetical habitable era for Venus's later evolution. As a result, our models are agnostic to Venus's formation, initial composition, magma ocean evolution, and the details of the habitable era itself. Our O_2 loss model tracks the post-habitable-era evolution of H_2O, CO_2, and O_2 in Venus's atmosphere. We assume that all surface liquid water present immediately before the end of habitability enters the atmosphere, either during a runaway greenhouse (RGH) phase or a moist greenhouse phase, both of which could be triggered by the Sun brightening over time, or the outgassing of CO_2 through volcanism. We identify regions of parameter space using a regular grid of seven parameters where the water (and therefore oxygen) added to Venus's atmosphere by the evaporation of habitable era surface liquid water and subsequent volcanic H_2O outgassing can be removed by (Fig. 1):

1. Nonthermal O escape
2. Oxidation of degassed CO and CH_4 to CO_2
3. Oxidation of lava, ash, and magma.

Model runs are considered successful when the final atmospheric O_2, H_2O, and CO concentrations satisfy the upper limits on O_2, H_2O, and CO concentrations in Venus's modern atmosphere (26). We consider hypothetical habitable eras ending

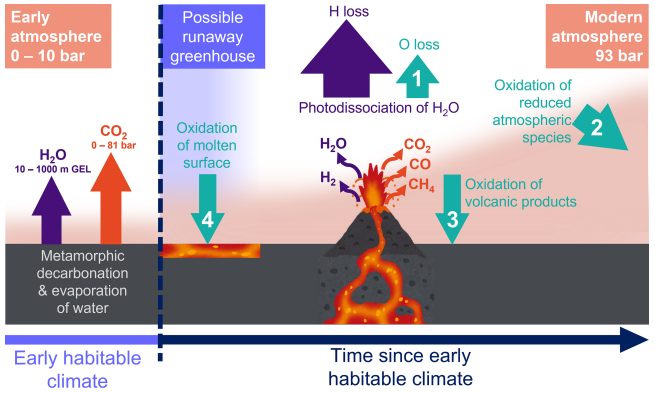

Fig. 1. Schematic illustration of our model for Venus's atmospheric evolution starting from the end of a hypothetical early habitable era. Prior to the model start, we set the total end-habitable-era water inventory (Table 1). After the end of the habitable era, the following processes occur: 1) Additional volatiles are added to the atmosphere by volcanism. These volatiles are sourced from H and C species dissolved in the melt, and their speciation into H_2O, H_2, CO_2, CO, and CH_4 is set by the oxygen fugacity of the erupting melt. 2) Water from volcanism and the early habitable era photodissociates to form H and O_2. 3) H escapes to space (purple arrow). 4) O is removed from the atmosphere by escape to space, oxidation of reduced atmospheric species such as H_2, CH_4, and CO to form H_2O and CO_2, and oxidation of FeO in volcanic products (teal arrows). In models where the habitable era ends in a runaway greenhouse (RGH), O can also be removed from the atmosphere by oxidation of a molten basalt layer if the surface temperature exceeds the basalt solidus.

at 4.0, 3.0, and 1.5 Ga, with end-habitable-era water inventories between 10 and 1,000 m GEL over a total of 94,080 model runs (parameters in Table 1; 47,040 runs each for the moist greenhouse case and the RGH case where oxidation of a molten surface occurs).

Two important processes in our O_2 loss model are the oxidation of degassed C and H species and oxidation of basalt lava flows. These processes both depend on Venus's crustal production and degassing history, which is constrained by the modern abundance of ^{40}Ar in Venus's atmosphere. This is because ^{40}Ar is produced by the decay of ^{40}K in the crust and in the mantle, and ^{40}Ar can be released from the mantle to the atmosphere through degassing from volcanic eruptions and intrusions. ^{40}Ar formed from ^{40}K decay in the crust can diffuse through the crust into the atmosphere (27, 28). As little as 24% of the radiogenic ^{40}Ar in Venus's mantle has been degassed (27), assuming an Earth-like K abundance on Venus. We construct a simple ^{40}Ar degassing model following (27, 28) to determine whether the ^{40}Ar degassed by the crustal production histories used in our O_2 loss model falls within or below the $(1.61 \pm 0.54) \times 10^{16}$ kg range for ^{40}Ar abundance in Venus's modern atmosphere (28).

1. Results

A. O_2 Loss Model. Our baseline O_2 loss model considers three oxygen sinks (Fig. 1):

1. Escape to space
2. Oxidation of reduced atmospheric species (CO, CH_4, and H_2) from degassing
3. Oxidation of basaltic lava flows and ash.

Results for our baseline model show that these combined oxygen sinks are able to remove enough O_2 to make end-habitable-era water inventories of up to 300 m GEL ($\lesssim$10% of an Earth Ocean)

Downloaded from https://www.pnas.org by UNIVERSITY OF CHICAGO THE JOHN CRERAR LIBRARY on March 8, 2023 from IP address 128.135.55.25.

Table 1. Parameter values used in O_2 loss model (*Materials and Methods* for details)

Symbol	Description	Values	Units
t_0	End of the habitable era (and model start time) in Gyr before present	4 (habitable for $\leq$ 0.5Gyr) 3 (habitable for $\leq$1.5 Gyr) 1.5 (habitable for $\leq$3 Gyr)	Gyr
h_{hab}	Global Equivalent Layer (GEL) water released into the atmosphere at the end of the habitable era (includes surface water, groundwater, and any water from minerals dehydrated during transition out of habitable conditions)	10, 50, 100, 300, 500, 700, 1,000	m
c_{CO_2}	Concentration of CO_2 in Venusian basaltic melts	0.03, 0.05, 0.1, 0.2	wt%
c_{H_2O}	Concentration of H_2O in Venusian basaltic melts	0.001, 0.1, 0.2, 0.5, 700, 1,000	wt%
f_{volc}	Fraction of CO_2 in Venus's present atmosphere derived from post-habitable era volcanic degassing	0.1, 0.5, 0.9, 1.0	
f_{ext}	Fraction of magmatism that is extrusive (reaches the surface as ash or lava rather than crystallizing deep underground)	0.1, 0.3, 0.9, 1.0	
$log\, fO_2$	Oxygen fugacity of erupting melt relative to the fayalite–magnetite–quartz buffer	0, −1, −2, −3, −4	$log\, fO_2 \Delta$FMQ

We implement a regular grid approach so all parameter combinations are explored.

consistent with Venus' present atmosphere (Fig. 2). This volume of water would be readily supplied during Venus's formation, with estimates for Venus's initial water inventory ranging from around 0.5 to 5 Earth Oceans (29, 30). The upper limit results from larger end-habitable-era water inventories contributing more O_2 to Venus's atmosphere than can be accommodated by the combined oxygen sinks in our model. The most important sinks are oxidation of reduced atmospheric species and oxidation of lava/ash. The relative contributions of these sinks to O_2 removal depend on the oxygen fugacity of erupting melts on Venus and the melt CO_2 and H_2O concentrations, which determine the speciation of degassed volatiles. For higher oxygen fugacities (e.g., $\log f O_2$ = FMQ $\pm$ 0, where FMQ is the fayalite–magnetite–quartz buffer), oxidation of lava/ash is the largest oxygen sink because less CO and CH_4 are degassed. As melt oxygen fugacity decreases and CO/CH_4 degassing increases, oxidation of CO/CH_4 becomes the primary O_2 sink. However, it is difficult for oxidation of CO/CH_4 to exactly balance O_2 introduced by end-habitable-era water inventories. Ongoing H_2O degassing is required in these runs to provide a continuous supply of O_2 and prevent Venus' atmosphere from becoming too CO-rich to satisfy modern CO constraints.

An exception to this 300-m-GEL upper limit is if average melts on Venus have very reduced oxygen fugacities comparable to the most reduced Mars meteorite ($\log f O_2$ = FMQ−4, Fig. 3). Models of mantle oxygen fugacities resulting from a magma ocean suggest that Earth and Venus-sized worlds will have more oxidized upper mantles (31), and Earth's upper mantle has an

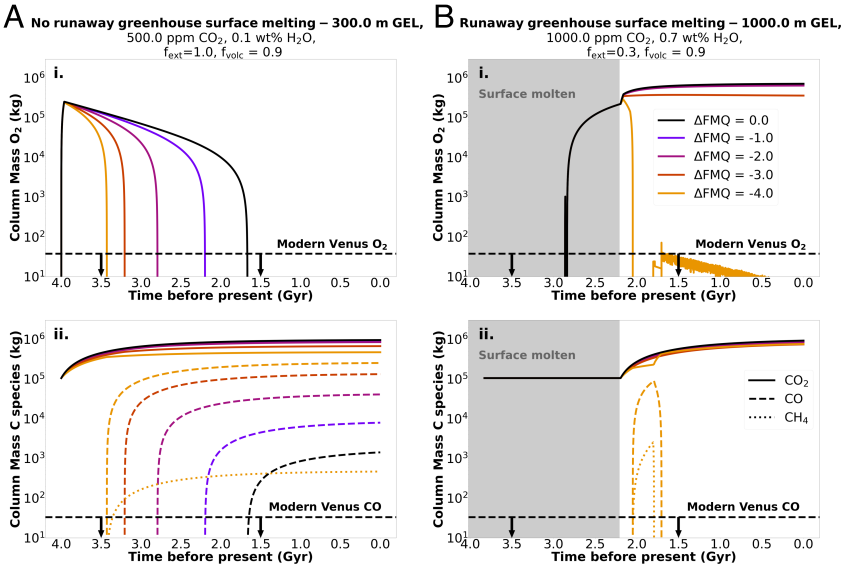

Fig. 2. Example model output: Melts with lower oxygen fugacity can enable larger end-habitable-era water inventories to be compatible with modern atmospheric composition; however, melts with low oxygen fugacities also outgas reduced gasses such as CO which can overwhelm the O_2 available to oxidize them and produce an atmosphere with far greater CO than observed on modern Venus. Time evolution of column masses of *i* O_2 and *ii* C species for different melt oxygen fugacities in a. our baseline model, with all early habitable eras ending with 300 m GEL 4.0 Ga ago and b. with 1000m GEL RGH surface melting. Line colors indicate melt oxygen fugacity. In *ii*, CO_2, CO, and CH_4 are indicated with solid, dashed, and dotted lines, respectively. Black dashed horizontal lines show upper limits for modern Venus O_2 (<70 ppm) and CO (<52 ppm) in *i* and *ii*, respectively (26). Only models that fall beneath both of these limits are considered successful.

Downloaded from https://www.pnas.org by UNIVERSITY OF CHICAGO THE JOHN CRERAR LIBRARY on March 8, 2023 from IP address 128.135.55.25.

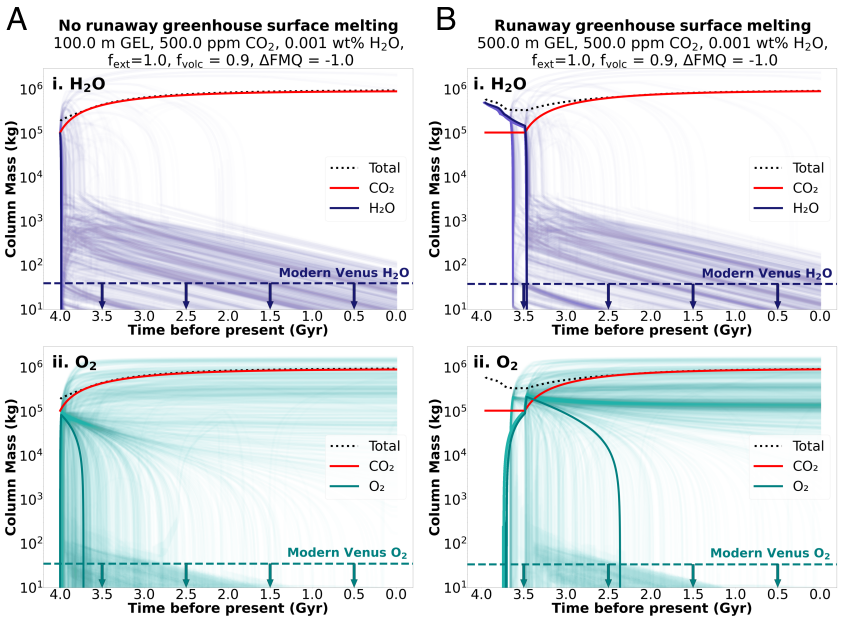

Fig. 3. Example model output: Time evolution of column masses of *i* H_2O (purple) and *ii* O_2 (teal) for (*A*) our baseline model, with all early habitable eras ending with 100 m GEL 4.0 Ga ago, and (*B*) with RGH surface melting, showing all habitable eras ending with 500 m GEL at 4.0 Ga. Where red CO_2 curve is flat, surface is molten and volcanism does not occur. Runs are shown as translucent lines. Solid lines illustrate cases where atmospheric evolution is compatible with modern atmospheric H_2O and O_2. Dashed purple lines show upper limits for modern Venus H_2O, and dashed teal lines show upper limits for O_2. Adding runaway greenhouse (RGH) surface melting to our models enables slightly larger end-habitable-era water inventories to be compatible with modern atmospheric H_2O and O_2.

oxygen fugacity around $\log fO_2$ = FMQ ± 0 (32). However, mantle oxygen fugacities as low as $\log fO_2$ = FMQ−4 have previously been proposed (12). For the $\log fO_2$ = FMQ−4, end-habitable-era water inventories as large as 1,000 m GEL (~33% of an Earth ocean) remain consistent with Venus's modern atmosphere in our models, provided that melt H_2O

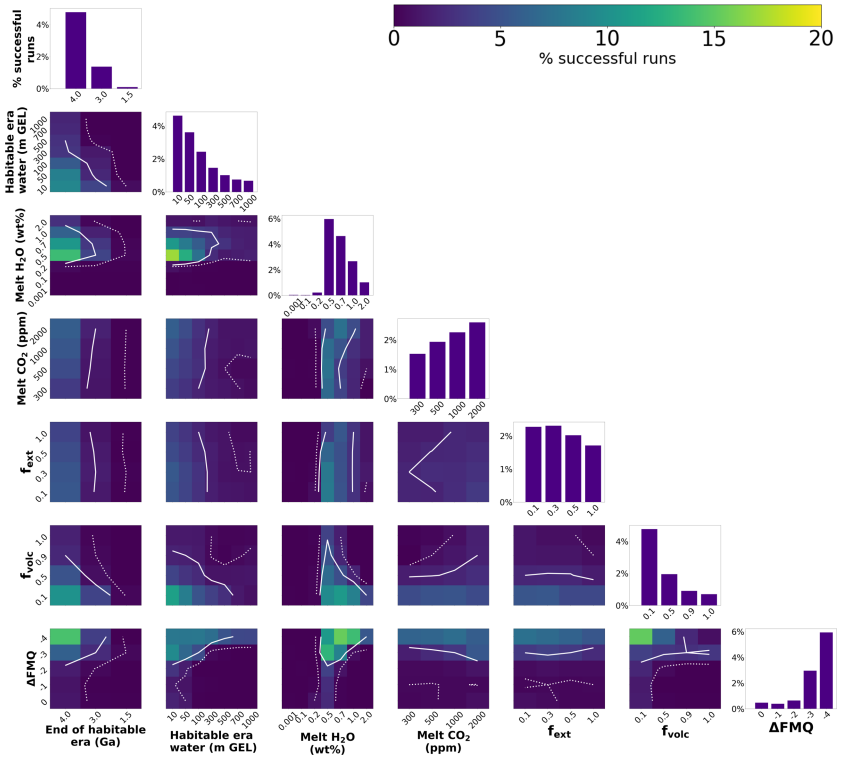

Fig. 4. Percentage of model runs that end with atmospheric H_2O, O_2, and CO concentrations consistent with data for modern Venus (25) for different combinations of parameters (Table 1) for runs without runaway greenhouse (RGH) surface melting. Contour plots show model success rates for combinations of different values of 2 parameters. Dashed and solid white lines indicate 2σ and 1σ levels, respectively. Summary bar charts show model success rates for different values of a single parameter. f_{ext} is the extrusive magmatism fraction, f_{volc} is the fraction of Venus's modern atmospheric CO_2 derived from post-habitable era volcanic degassing, and $\log fO_2$ ΔFMQ is the oxygen fugacity of erupting melts since the end of the habitable era relative to the fayalite–magnetite–quartz buffer.

Downloaded from https://www.pnas.org by UNIVERSITY OF CHICAGO THE JOHN CRERAR LIBRARY on March 8, 2023 from IP address 128.135.55.25.

concentration is >0.2 wt%. Model runs with 10-m-GEL end-habitable-era water—an ocean three hundred times shallower than Earth's—can evolve to be at or below Venus's present-day atmospheric O_2 levels for 5% of 10 m GEL runs overall; (Figs. 2*A*, 4*A*, and 5). A 10-m-GEL end-habitable-era water inventory is the only case for which low modern atmospheric O_2 concentrations can be matched by habitable eras ending as late as 1.5 Ga.

When $\log fO_2$ ≥FMQ−3, 300-m-GEL end-habitable-era water inventories are compatible only with Venus's modern atmosphere in runs where the habitable era ends early, at or before 3.0 Ga (Fig. 4 and *SI Appendix*, Fig. S1). In runs with habitable eras that end early in Venus's history, the Sun's X-ray/extreme ultraviolet (XUV) flux is high and can drive rapid H escape causing rapid buildup of O_2 in the atmosphere. This is advantageous because the volcanism rate decreases exponentially with time in our models, so oxidizable basalt—which can be a major oxygen sink—is most available soon after the end of the habitable era. An early end to the habitable era allows basalt oxidation to sequester the most O_2, as O_2 is available to be removed at the time of eruption.

When we add RGH surface melting to our baseline O_2 loss model, end-habitable-era water inventories ≥300 m GEL permit surface temperatures hot enough to melt basalt, enabling rapid diffusion of oxygen into a basaltic surface magma layer. This RGH is caused by vaporization of the end-habitable-era water inventory and is distinct from a steam atmosphere formed during accretion (33). The surface magma layer provides an additional O_2 sink as long as the H_2O greenhouse effect melts surface basalt (34). However, adding this additional O sink only increases the total number of successful O_2 loss model runs from 2.2% to 2.6% (Figs. 2*B*, 4*B* and 5).

This is because:

1. In runs with large water inventories but little initial atmospheric CO_2, the surface magma layer is short lived because H_2O loss rapidly reduces the greenhouse effect. This leads to a short-lived and thin surface magma layer that consumes only remove a small amount of O_2.
2. In runs with large water inventories and a large fraction of Venus's modern atmospheric CO_2 degassed prior to the end of the habitable era, H loss is slow because it must diffuse through a thick background atmosphere. This extends the lifetime of the oxidizable magma layer but delays accumulation of atmospheric CO_2 because we do not include volcanic outgassing while the surface is molten. For habitable eras ending at 4.0 and 3.0 Ga, the surface magma layer can persist so long that it is no longer possible for all of Venus's present-day CO_2 to volcanically degas after the surface of the magma layer freezes.
3. For habitable eras ending at 1.5 Ga and water inventories of 1,000 m GEL, the increase in bolometric insolation and decrease in H loss rates due to the Sun's reduced XUV output (35) enable a H_2O greenhouse with a surface magma layer to last until the present, which is inconsistent with data.
4. In runs with reducing melts, removal of atmospheric O_2 leftover from H escape of the end-habitable-era water inventory can remove so much O_2 from the atmosphere that there is no longer enough oxidizing power available to oxidize degassed CO and CH_4 fully to CO_2, leading to final atmospheric CO concentrations too high to match Venus's modern atmosphere.

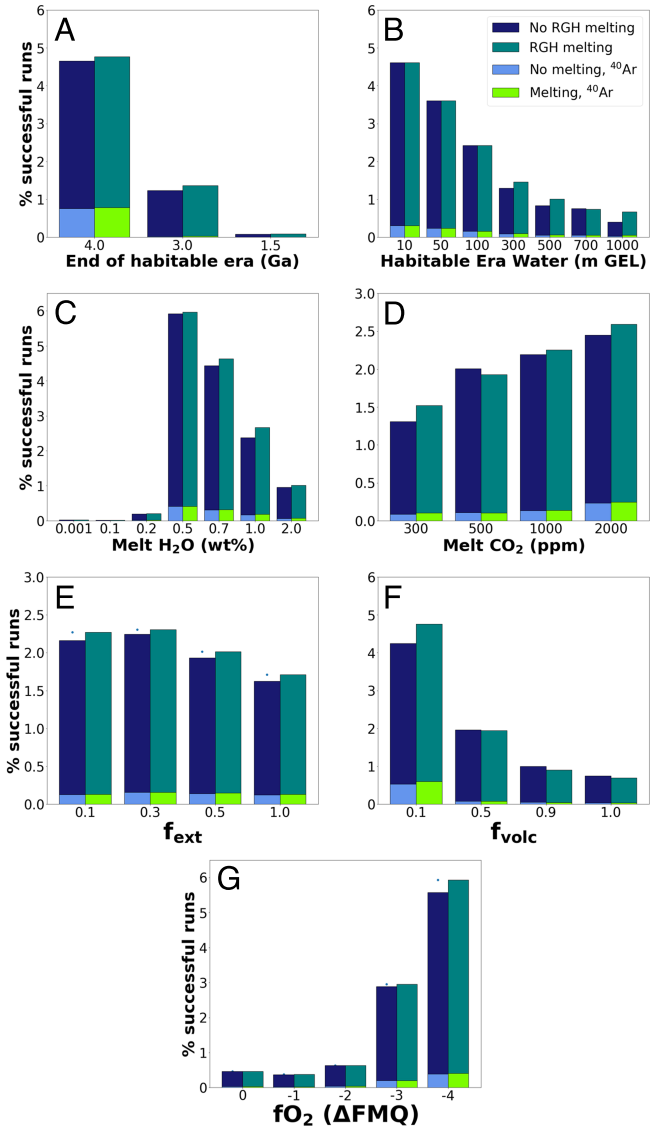

Fig. 5. Comparison of fraction of successful runs (runs that have final atmospheric O_2, H_2O, and CO concentrations less than upper limits for Venus's present atmosphere) compatible with modern Venus atmosphere for models without runaway greenhouse (RGH) melting (dark blue) and with RGH melting (dark green). Successful runs that also fall within or below the range of Venus's modern atmospheric ^{40}Ar abundance are also shown for models with (light blue) and without (light green) RGH. All parameter values correspond to Table 1.

B. ^{40}Ar Degassing Model. Oxidation of the degassed atmospheric species CO and CH_4 and oxidation of lava flows are the most important oxygen sinks in our baseline model. During degassing and volcanism, minor atmospheric constituents such as ^{40}Ar are released into the atmosphere alongside major C and H species and can be used to place constraints on the total crustal production on Venus (27, 28). We model the ^{40}Ar degassing corresponding to the crustal production histories used in our O_2 loss models.

Overall, ≲0.4% of runs are consistent with Venus's present-day atmospheric O_2 and ^{40}Ar for the parameter ranges investigated in this study. To match modern Venus's low atmospheric ^{40}Ar, our ^{40}Ar degassing model requires parameters that minimize the total production of new crust (Fig. 5 and *SI Appendix*, Fig. S4). High melt fractions reduce the concentration of ^{40}K and ^{40}Ar in mantle-derived melts, reducing the amount of ^{40}Ar degassed directly to the atmosphere during volcanism and the

Downloaded from https://www.pnas.org by UNIVERSITY OF CHICAGO THE JOHN CRERAR LIBRARY on March 8, 2023 from IP address 128.135.55.25.

amount of ^{40}K available in the crust to decay and also supply ^{40}Ar to the atmosphere. Thin crust promotes rapid recycling of ^{40}K-enriched crust back into the mantle, reducing the amount of time available for crustal ^{40}K to decay and release ^{40}Ar to the atmosphere through the crust for a given crustal production rate. Low values of f_{volc}—which correspond to most of Venus's modern CO_2 degassing before the end of a hypothetical habitable era—reduce the total amount of CO_2 that needs to be degassed during the model runs, which in turn reduces the necessary crustal production and the total amount of mantle melting and degassing required to achieve Venus's modern CO_2 atmosphere. This is advantageous for satisfying the ^{40}Ar constraint because earlier degassing leaves less time for ^{40}K to decay, so the atmosphere by the end of the habitable era can have abundant CO_2 but still be ^{40}Ar poor. However, reducing the total crustal production (advantageous for matching the ^{40}Ar constraint) reduces the size of the basalt lava flow oxidation and degassed reduced species O_2 sinks.

Together, these factors make it more difficult to reconcile a hypothetical early habitable era with data for modern Venus and narrow the range of parameters that reconcile a hypothetical habitable era with measurements of Venus's modern atmosphere. Within the framework of our model, only a small loophole in parameter space, corresponding to less than 0.4 % of model runs, remains when the ^{40}Ar and oxygen constraints are combined (light blue and light green columns in Fig. 5):

1. The habitable era must end prior to 3 Ga: In our models, volcanism is required to supply fresh basalt and reduced gases (particularly CO and CH_4) to Venus's surface and atmosphere to act as an oxygen sink. The later in Venus's history this volcanic activity occurs, the longer mantle ^{40}K has to decay into ^{40}Ar, which is then degassed during volcanism. Extensive ^{40}Ar degassing in runs violates the observed low ^{40}Ar in Venus's modern atmosphere. Therefore, within the framework of our model, Venus must have been uninhabitable for at least ~70% of its history, >4 times as long as some previous estimates (8).
2. The end-habitable-era water inventory must be ≤300 m GEL, unless melt oxygen fugacity $\log fO_2$ less than FMQ−3: For more oxidized average melts on Venus, oxygen sinks in our model can remove only the O left behind by H escape from 300 m GEL of water at the end of a habitable era. When erupted melts have lower oxygen fugacities, the corresponding increase in degassed CO and CH_4 can remove an additional 500 m GEL or more. Therefore, within the framework of our model, if Venusian melts have similar oxygen fugacity to mid-ocean ridge (MOR) melts on Earth, i.e., $\log fO_2 \approx$FMQ±4 (32), Venus's oceans were shallow by the end of the habitable era.
3. Average melts erupted on Venus after the habitable era must have had ≥0.2wt% dissolved H_2O, unless Venus melts have high oxygen fugacities: Oxidation of degassed CO and CH_4 is a major O_2 sink in our baseline model. Degassing of reduced species continues after all O_2 is consumed. As a result, degassing of CO and CH_4 often exceeds the O_2 reduction sink. Continued H_2O degassing through Venus's post-habitable history provides a supply of O_2 as H escapes to space to balance continued CO and CH_4 degassing. A given model run typically behaves in one of two ways: 1. Venus's post-habitable evolution does not have sufficient O_2 sinks to remove O_2 from the atmosphere to match modern constraints. 2. Once O_2 from a large end-habitable-era water inventory is depleted in a run with larger cumulative O_2 sinks caused by either a surface melt layer during a runaway greenhouse or abundant extrusive volcanism, the O_2 available to oxidize CO and CH_4 to CO_2 has been used up, and degassed CO accumulates rapidly in the atmosphere. In other words, exactly matching the reducing capacity of the Venus surface–atmosphere system to the oxygen introduced by loss of an end-habitable-era H_2O inventory and degassed water requires fine-tuning.

Only ~10% of our 57,600 total ^{40}Ar degassing model runs (independent of our oxygen loss runs) fall within or below the measured range for Venus's modern atmospheric ^{40}Ar abundance. However, many of the ^{40}Ar degassing runs that can reproduce Venus's modern ^{40}Ar abundance have parameter combinations that cannot reproduce Venus's modern O_2, H_2O, and CO concentrations in our O_2 loss model. This reduces the proportion of our O_2 loss runs that are consistent with Venus's present-day atmosphere when both oxygen and ^{40}Ar are considered to be less than 0.4% (Fig. 5).

2. Discussion

A. Evolution of Habitable Era Surface Water Inventory. Our models place an upper limit of 500 m GEL on the total water inventory supplied to the atmosphere at the end of a hypothetical habitable era on Venus, unless Venus's eruptive history has been dominated by melts with an oxygen fugacity of $\log fO_2$ less than FMQ−3 in which case the end-habitable era inventory can extend to 1,000 m. Our O_2 loss model constrains only the final water inventory before conditions transitioned from habitable to uninhabitable. However, the surface water inventory during a hypothetical habitable era need not be constant. To quantify the evolution of a hypothetical habitable era's water inventory over time, we model the hydration of crust and the recycling of hydrated crust into the mantle.

We constructed a steady-state 1-D model (*Materials and Methods*) of the simplest possible case where Venus's crust is recycled in a vertical conveyor belt-like fashion (36, 37). New lava erupted at the surface buries older crust, which will eventually subside into the convecting mantle (36). For a given lithospheric thickness and eruption rate (which we assume to be constant throughout the habitable era for this exercise), we find the geotherm through the lithosphere (38, 39). We compare this geotherm to phase boundaries for eclogite formation (40) and serpentinite dehydration (41). When dense eclogite forms, the crust is more likely to sink into the mantle (37). Where the geotherm encounters the eclogite stability field before serpentine dehydrates, we assume that the hydrated lithosphere returns water to the mantle through entrainment in convection (42). When the geotherm crosses into the serpentinite dehydration field first, water is returned to the surface or shallow crustal reservoirs and not into the mantle. We investigate a range of internal radiogenic heating rates comparable to those observed in modern terrestrial basalts (43). Higher internal radiogenic heating rates (e.g., adjusted for a younger planet with a higher concentration of decaying radioactive elements) generate geotherms with crusts thinner than 5 km, which is the lowest crustal thickness we consider in this model based on the range estimated for modern Venus (44). These thin, hot crusts do not pass through the eclogite stability field and, therefore, do not lead to recycling of hydrated crust into the mantle within the framework of our

Downloaded from https://www.pnas.org by UNIVERSITY OF CHICAGO THE JOHN CRERAR LIBRARY on March 8, 2023 from IP address 128.135.55.25.

model. Lithospheres thicker than 100 km with internal heating rates less than 5 $\mu W\ m^{-3}$ (*SI Appendix*, Fig. S5) are able to form eclogite before serpentinite dehydration occurs.

Next, we model the time-evolving surface water inventory during a hypothetical habitable era on Venus (*Materials and Methods*) only for the cases where water recycling into the mantle is able to occur, starting from inventories as large as 3,000 m GEL, or 1 Earth ocean. At each timestep, we use Venus's present-day topography to approximate the corresponding proportion of Venus's surface that would be submerged. Submerged areas of the surface are permitted to form a hydrated crust (0.1 to 3 wt% H_2O) (12, 45), with lithospheric recycling occurring at the same rate as crustal production. To maximize the water removed from the surface inventory, which maximizes the peak depth of a hypothetical ocean on early Venus, we assume that all crustal production occurs as extrusive volcanism. We also track H_2O release by volcanic degassing (*Materials and Methods*).

In some cases, the surface water inventory approaches a steady state where removal by burial of hydrated crust (occurring at a rate set by the surface water inventory and crustal production rate) matches water inputs by volcanic degassing. Models with low ($\leq$0.2 wt%) melt H_2O concentrations do not reach a steady state and instead lose all of their water (*SI Appendix*, Figs. S7 and S8).

In order for a habitable era with an evolving surface water inventory to be compatible with our O_2 loss and ^{40}Ar degassing model results, the surface water inventory by the end of the habitable era must be below 500 m GEL (Fig. 5). This is favored by melt H_2O concentrations between 0.1 and 0.7 wt% and high mass fractions ($\geq$0.5 wt%) of water in hydrated crust (*SI Appendix*, Figs. S7 and S8). For cases where the final water inventory drops below 500 m GEL, the average surface water inventory over the course of the habitable era can be up to half an order of magnitude greater than the final water inventory for a few combinations of crust hydration and melt H_2O concentration, allowing for much deeper oceans on early Venus in some cases. However, this mechanism for net sequestration of water in the mantle through burial of hydrated crust does not affect the conclusion that only hypothetical habitable eras that ended prior to 3 Ga are consistent with ^{40}Ar, O_2, H_2O, and CO concentrations in Venus's modern atmosphere (26, 28).

B. Limitations. The paucity of existing data for modern Venus severely restricts our understanding of Venus's past. This is one of the primary drivers for Venus exploration over the coming decades. It is currently unknown whether Venus has ongoing volcanism, what the planet's tectonic regime is, how thick the crust and lithosphere are, what the mantle composition is—let alone how all of these important factors have evolved over the past 4 Gyr (46). As a result, our treatment of Venus's post-habitable evolution in both our oxygen loss and Ar degassing models is highly simplified.

First, to enable modeling with the least number of assumptions about Venus's interior, we have assumed that the composition of melts erupting on Venus does not change over time. Thus, we model "average" melts on Venus. Eruptions resulting from mantle plumes (46) or local magmatic systems may have different volatile concentrations.

Second, we do not include degassing of S to reduce the number of parameters needed to describe melt compositions and degassing. Although this has a negligible impact on the speciation of the gasses included in our model (47), Venus's modern atmosphere contains SO_2, SO, and other S species. This requires that Venus has recently degassed—and may still be degassing—S in some form (48). It follows that oxidation of S species may have acted as an O_2 sink analogous to the way oxidation of CO to CO_2 is an important mechanism for removing atmospheric O_2 in our model.

Third, our approach to modeling surface melting during a runaway greenhouse is highly simplified. To maximize the potential oxygen sink, we assume that diffusion of oxygen into the melt does not limit the rate at which the melt oxidizes such that all molten material at a given timestep is available to oxidize. Our approach also neglects the greenhouse effect of CO_2. CO_2 contributes around 420 K of greenhouse warming to Venus's modern atmosphere (49), which is not sufficient to melt Venus's surface under the bright modern Sun, and much less than the maximum greenhouse warming possible under the same insolation with H_2O (34). Additionally, the absorption bands for CO_2 and H_2O overlap, so their greenhouse effects are not additive (50). Our modeling approach focuses on the feedback between the much stronger H_2O greenhouse effect and H escape to space; however, this may underestimate the surface temperature at a given timestep, which could extend the duration of the runaway greenhouse melting stage and lead to greater O_2 loss.

Fourth, we assume that Venus's eruptive history can be modeled as an exponential decay between the end of the habitable era and the present day. The crater retention age of Venus's surface suggests that the planet has been resurfaced geologically recently (51, 52). This crater retention age can be explained by either a catastrophic resurfacing event 0.3 to 1 Gyr ago (53) or equilibrium resurfacing by continuous volcanism (54). We opt for continuous volcanism in our models because this maximizes the lava flow oxidation oxygen sink by erupting fresh lava, rather than having surface oxidation limited by diffusion. This, in turn, maximizes the end-habitable-era water inventory possible in our models, which is conservative relative to our conclusion that only a narrow range of parameters is consistent with Early Venus habitability. Differences in Venus's crustal production history will not change our fundamental conclusion that the reducing power introduced to Venus's surface–atmosphere system by nonthermal O escape, eruption of lava flows containing minerals that can be oxidized, and degassing of gasses such as CO and CH_4 must balance the total O_2 introduced by H escape from an end-habitable-era water inventory and any subsequently degassed H_2O in order to reconcile a past habitable era with Venus's modern atmosphere. However, differences in Venus's crustal production history are important for ^{40}Ar degassing. Our approach is also conservative with respect to ^{40}Ar degassing because degassing is greatest earlier in our models, reducing the time for ^{40}K decay to make ^{40}Ar available in the mantle for release by volcanism.

Fifth, our ^{40}Ar degassing model is based on a large number of poorly constrained parameters (*SI Appendix*, Table S2) and requires assumptions about Venus's tectonic regime and prehabitable era evolution. There are several potential ways to reduce ^{40}Ar degassing over Venus's history that could make a larger proportion of our model results consistent with Venus's modern atmospheric composition. For example, the concentration of radioactive isotopes in Venus's mantle is poorly constrained (27). A lower concentration of U and K in Venus's mantle would reduce the accumulation of ^{40}Ar in the mantle and therefore ^{40}Ar degassing over time. Additionally, ^{40}Ar may not be distributed homogeneously through Venus's mantle. If Venus has mantle reservoirs enriched in incompatible elements or a thick basal magam occan (55), ^{40}Ar may be prevented from degassing to the

Downloaded from https://www.pnas.org by UNIVERSITY OF CHICAGO THE JOHN CRERAR LIBRARY on March 8, 2023 from IP address 128.135.55.25.

atmosphere, increasing the number of our model runs compatible with Venus's modern atmospheric ^{40}Ar concentration.

C. Implications for Upcoming Venus Missions. Our model results suggest, in agreement with previous results (12), that a habitable era on Venus with abundant surface liquid water was unlikely and suggest a number of tests for upcoming Venus missions: VERITAS (Venus Emissivity, Radio science, InSAR, Topography, And Spectroscopy), DAVINCI (Deep Atmosphere Venus Investigation of Noble gases, Chemistry, and Imaging), and EnVision.

For example, VERITAS high-resolution topography and gravity data could be used to better constrain Venus's present lithospheric thickness. At present, this parameter is not well enough constrained to distinguish between a range of possible tectonic regimes. Our results favor a tectonic regime with limited volcanism over the past 4 Gyr to reconcile any early habitable era with Venus's modern atmosphere. Determining Venus's modern (or recent) tectonic regime and lithospheric thickness is also important for better constraining ^{40}Ar degassing models, by providing constraints on the recycling depth of ^{40}K-enriched crust.

Both VERITAS and DAVINCI will survey high SiO_2 rocks on Venus's surface. If these rocks resemble terrestrial andesites and rhyolites, this could imply H_2O in the melting zone and suggest high melt H_2O concentrations consistent with our successful model runs (56, 57). However, hydrous melting will need to be distinguished from anhydrous fractional crystallization processes, which can also produce silicic magmas (57).

VERITAS also plans to measure FeO abundance. This can be used to narrow down the range of likely melting conditions and extent of fractional crystallization on Venus (58), which also constrain melt volatile concentrations. Crustal FeO abundance can also be used to refine the estimate of the FeO concentration in Venusian basalts used in our models. If Venus's FeO is very high, this will increase the oxidizing potential per unit volume of lava, thus potentially driving our results toward higher required melt H_2O concentrations to compensate for greater loss of atmospheric O_2 to oxidizing Venus's basaltic surface while atmospheric O_2 is greatest early in Venus's post-habitable evolution.

3. Conclusions

Nonthermal O escape to space, oxidation of basaltic lava flows, and oxidation of degassed CO and CH_4 can remove oxygen from up to 300 m GEL on the total water inventory supplied to the atmosphere at the end of a hypothetical habitable era on Venus, unless Venus's eruptive history has been dominated by melts with an oxygen fugacity of $\log fO_2$ less than FMQ−3 Earth MORB is around $\log fO_2$ = FMQ ± 0 (32), in which case the end-habitable era inventory can extend to 1,000 m. The oxidation of a transient layer of basaltic melt during an end-habitable-era runaway greenhouse (RGH) can remove oxygen corresponding to an additional 200 m GEL of water (Figs. 4 and 5), raising the limit to 500 m GEL for Venus histories with melt oxygen fugacities $\log fO_2 \geq$FMQ−3. Although these results reconcile a potential early habitable era on Venus with the paucity of O_2 in Venus's modern atmosphere, only 2.6% of parameter combinations in our models lead to post-habitable era outcomes that satisfy atmospheric abundance data for modern Venus. These successful runs define a narrow loophole in parameter space where the reducing power of the Venus surface–atmosphere system since the end of a habitable era is able to balance the O_2 introduced by the escape of H from end-habitable-era water and degassed H_2O.

This loophole becomes even smaller when additional constraints on Venus's history are taken into consideration. The two most important oxygen sinks in our models are oxidation of degassed CO and CH_4 and oxidation of basaltic lava flows, both of which require volcanism and degassing on Venus since the end of a hypothetical habitable era. Degassing and volcanism due to crustal production on Venus lead to degassing of ^{40}Ar. When the ^{40}Ar contributions to the atmosphere caused by the eruption of lava flows and degassing needed to remove oxygen from Venus's atmosphere through oxidation of basaltic volcanic products and reduced gasses like CO and CH_4 are taken into account, only models with habitable eras ending before 3.0 Ga are consistent with ^{40}Ar, O_2, H_2O, and CO measurements of Venus's modern atmosphere (Fig. 5), reducing the success rate of our models to less than 0.4% of model runs.

Although our modeling results demonstrate that Venus must have had less than 500 m GEL water by around 4 Ga unless Venus's average melts had oxygen fugacities comparable to that of the most reduced Martian meteorite, we also find that the time-averaged water inventory on an early habitable Venus may have been much greater than this upper limit. Efficient recycling of hydrated basaltic crust into the mantle through eclogite formation (40) might act to reduce Venus's surface water inventory during a habitable era. A 1-D model of this process suggests that habitable era averaged water inventories up to 1,000 m GEL could be consistent with our O_2 loss and ^{40}Ar degassing modeling results even for melts with higher oxygen fugacities (*SI Appendix*, Figs. S7 and S8), provided that Venus had a lithosphere greater than 100 km thick with internal radiogenic heat production rates less than 5 $\mu W\ m^{-3}$ (*SI Appendix*, Fig. S6).

Key measurements for the VERITAS, DAVINCI, and EnVision missions that would help further evaluate the likelihood of a past habitable era (based on our modeling results) are lithospheric thickness and crustal SiO_2 and FeO abundances. For example, if hydrous melting is found to have been a significant process on Venus, this would support the existence of a past habitable era on Venus because our results suggest that high average melt H_2O concentrations are an important factor for preventing accumulation of abundant CO in Venus's atmosphere.

Materials and Methods

We combine simple models of degassing of basaltic melts (59), atmospheric escape of H and O, and removal of O from the atmosphere by oxidation of reduced gases, lava flows, and ash (when formed) to track the evolution of Venus's atmospheric composition since the end of an early habitable period using a 4th-order Runge–Kutte integration scheme. To identify post-habitable era scenarios that are compatible with Venus's present-day atmospheric composition, we vary seven key parameters in our model (Table 1) with each parameter value weighted equally. All parameter combinations resulting in final atmospheric H_2O, O_2, and CO concentrations below upper limits (25) for Venus's atmosphere are marked as "successes."

A. Initial Conditions. Each model begins at time t_0, after the end of a hypothetical early habitable era on Venus. The initial column mass of CO_2 is

$$M_{CO_2,0} = (1 - f_{volc}) M_{CO_2,f}, \quad [1]$$

where f_{volc} (Table 1) is the fraction of CO_2 in Venus's present-day atmosphere from post-habitable era volcanic degassing, and $M_{CO_2,f}$ is the column mass of CO_2 on Venus today. We consider values of f_{volc} greater than 0.1 because we assume that some CO_2 must be degassed after the end of a habitable era due to Venus's young surface age (51, 52). We extend the range to $f_{volc} = 1$

Downloaded from https://www.pnas.org by UNIVERSITY OF CHICAGO THE JOHN CRERAR LIBRARY on March 8, 2023 from IP address 128.135.55.25.

because a habitable atmosphere on Venus may have been CO_2 poor, as Earth's is today. Any CO_2 present at t_0 is assumed to have degassed prior to/during the habitable era, or through metamorphic decarbonation during the transition from habitable to uninhabitable conditions (36, 60, 61).

We also initialize our model with H_2O added to the atmosphere by vaporization of any surface liquid water present during the habitable era (Table 1). We consider water inventories between 10 and 1,000 m GEL. Our lower limit is based on water inventories required to sustain habitable surface temperatures in existing Venus climate model studies (8). The loss of up to 3,000 m GEL of water, or 1 Earth ocean, is one interpretation of Venus's modern D/H ratio (14, 15). We treat the initial atmospheric water in two different ways, corresponding to two different ways that water could have entered Venus's atmosphere during and at the end of a hypothetical habitable era. First, we consider a case where atmospheric water vapor does not lead to surface melting. This corresponds to a moist greenhouse where H is lost to space via a moist stratosphere (62), but the surface remains too cold to melt basalt. For simplicity, we do not explicitly model the time evolution of the moist greenhouse phase and, instead, assume that all H from the starting water inventory has already escaped, leaving behind O_2. Second, we consider a case where greenhouse warming from H_2O vaporized during an RGH causes melting of Venus's surface. We calculate surface temperatures as a function of partial pressure of water vapor in the atmosphere (34). This enables us to quantify the potential importance of oxidation of a surface magma layer as an O_2 sink.

Runaway greenhouse. Post-habitable era surface temperatures on Venus may have exceeded the melting point of rock. For atmospheric water inventories as small as 0.1 Terrestrial Oceans (TO) and a solar flux twice that of present-day Earth, temperatures can exceed 2,000 K (34). Diffusion of oxygen into surface magma could oxidize Fe^{2+} to Fe^{3+}, serving as an O_2 sink. The duration of this O_2 sink depends on initial atmospheric water inventory and the combined H escape rate and dissolution of H_2O in the melt. These two processes both deplete atmospheric H_2O vapor, which reduces the surface temperature (the greenhouse effect of O_2 is negligible). We find surface temperature at each timestep, given the incoming solar flux relative to Earth's insolation (S_{eff}) and partial pressure of H_2O in the atmosphere in bars (p_{H_2O}), using an equation fit to existing numerical results (63) (*SI Appendix, Oxygen Loss Model* and Table S1). We neglect the greenhouse effect of background CO_2. The parameters that determine Venus's evolution during RGH melting are t_0, h_{hab}, f_{volc}, and f_{ext} (Table 1), so for computational efficiency, we model RGH evolution separately until the surface melt layer freezes and then input the results as starting conditions for our baseline model.

To calculate removal of oxygen by oxidation of Fe^{2+} in basaltic melt at the surface, we calculate the temperature-depth profile of a 50-km thick crust at each timestep as the surface temperature evolves using a 1-D finite difference method. In the absence of any constraints on the crustal thickness on early Venus, we choose a maximum crustal thickness of 50 km because this is the thickness of basaltic crust required to remove the oxygen produced by the escape of 1 Earth ocean of water (64), which exceeds the maximum habitable-era water inventory considered in our models. Temperature within the crust evolves by diffusion:

$$\rho c_p \frac{\partial T}{\partial t} = \frac{\partial}{\partial z}\left(k\frac{\partial T}{\partial z}\right) - q_L, \qquad [2]$$

where q_L is heat flux due to the latent heat of fusion:

$$q_L = \rho L \frac{\partial z_{melt}}{\partial t}, \qquad [3]$$

where z_{melt} is the effective magma layer thickness produced at each depth in the model. Our upper boundary condition in the model is the surface temperature, which is a function of insolation and water vapor in the atmosphere. We impose a heat flux of 50 mW m^{-2} as our lower boundary condition.

As the thickness of the melt layer and the partial pressure of H_2O in the atmosphere evolve, so does the amount of H_2O stored in the melt layer. As H escapes to space and as the melt layer thickens, less H_2O dissolves in the melt because the partial pressure of H_2O is reduced. However, as the melt layer refreezes and partial pressure of H_2O drops, H_2O can also be re-exsolved into the atmosphere. The solubility of H_2O in the runaway greenhouse-triggered surface melt ($s_{H_2O,RGH}$) at a given timestep is (65):

$$s_{H_2O,RGH} = 3.44 \times 10^{-8} P_{H_2O}^{0.74},$$

where P_{H_2O} is the partial pressure of H_2O in the atmosphere.

$$P_{H_2O} = \frac{n_{H_2O,atm}}{n_{atm}} p_{atm}, \qquad [4]$$

where $n_{H_2O,atm}$ is the number of moles H_2O per column mass in the atmosphere, n_{atm} is the total number of moles in the atmosphere, and p_{atm} is the total atmospheric pressure. We assume that dissolved H_2O is mixed throughout the melt layer and that the dissolved H_2O content adjusts to match the H_2O solubility. Therefore, the change in atmospheric H_2O at each timestep is given by:

$$\frac{\partial n_{H_2O,atm}}{\partial t} = -\frac{\rho_{melt}}{m_{H_2O}} \frac{\partial}{\partial t}\left(s_{H_2O,RGH} z_{melt}\right). \qquad [5]$$

To calculate O_2 losses due to melt oxidation, we compute the melt fraction of a basalt with major element composition given by the Venera 14 surface measurements at a range of temperatures and pressures using alphaMELTS (66–68). We use these model runs to generate a lookup table which we use to find melt fraction as a function of depth at each timestep. We assume that all Fe^{2+} in the melt can be completely oxidized, i.e., that O_2 can pervade the entire magma layer, for example, by small-scale convection. We track both the cumulative melt fraction ($f_{m,c}$) and the cumulative oxidized melt fraction ($f_{o,c}$) at each depth in the model. The oxidized melt fraction at each timestep is given by the following:

$$f_{o,c} = \frac{0.25 f_{m,c} \rho c_{FeO}}{n_{O2,atm}}, \qquad [6]$$

where $n_{O2,atm}$ is the number of moles of O_2 per column atmosphere. The factor of 0.25 accounts for the stoichiometry of Eq. **17**. $f_{o,c}$ at a given depth is not allowed to exceed 1.

B. Atmospheric Escape.

H escape. The bulk composition of Venus's atmosphere evolves throughout our models based on expressions for escape of H from Venus (69) which we use to track the accumulation of O_2 in the atmosphere. H is supplied by photodissociation of H_2O. Following previous work, we assume that the photodissociation rate does not limit H escape (62). Escape of a light species is limited by its ability to diffuse through the background atmosphere of heavier species that are not undergoing escape (23). At high H_2O mixing ratios, H escape approaches the XUV (energy) limit (Eq. **10**). At each timestep in our model, we calculate the diffusion-limited escape and the energy-limited escape of H and apply the lowest of the two.

The diffusion limit determines the maximum supply of the escaping species to the upper atmosphere. In this diffusion-limited case, the rate of atmospheric escape is

$$\dot{M}_{H,esc} = X_H \frac{GM_V(m_{atm} - m_H)}{R^2} \frac{b}{kT_{upper}}, \qquad [7]$$

where X_H is the molar mixing ratio of H in the atmosphere, and m_{atm} is the mean molecular weight of the background atmosphere, set by the molar ratio of non-H species after photodissociation has occurred:

$$m_{atm} = X_{CO_2} m_{CO_2} + 2X_{O2} m_O + X_{CO} m_{CO} + X_{CH_4} m_{CH_4}, \qquad [8]$$

and b is the diffusion coefficient of H in the background atmosphere, which depends on the abundance of other species (12, 69):

$$b_{H,atm} = \frac{b_{H\text{-}CO_2} X_{CO_2} + b_{H\text{-}CO} X_{CO} + b_{H\text{-}O} X_O}{X_{CO_2} + X_{CO} + X_O}, \qquad [9]$$

m_{CO_2}, m_{CO}, and m_{O_2} are the mean molar masses of CO_2, CO, and O_2, and X_{CO_2}, X_{CO}, and X_{O_2} are the mixing ratios of CO_2, CO, and O_2. $b_{H\text{-}CO_2} = 8.4 \times 10^{19} T_{upper}^{0.6}$, $b_{H\text{-}CO} = 6.5 \times 10^{19} T_{upper}^{0.7}$, and $b_{H\text{-}O} = 4.8 \times 10^{19} T_{upper}^{0.75}$

Downloaded from https://www.pnas.org by UNIVERSITY OF CHICAGO THE JOHN CRERAR LIBRARY on March 8, 2023 from IP address 128.135.55.25.

are the binary diffusion coefficients of H in CO_2, CO, and O, respectively, in mol m^{-1} s^{-1} (70, 71). Binary diffusion coefficients are derived from empirical fits to measured data and can deviate from the data by several tens of percent. To quantify the impact of this effect on our results, we conducted sensitivity tests with values of b_{atm} 30% lower and 30% higher than our baseline value and found that the total number of successful runs is not sensitive to ±30% variations in the binary diffusion coefficient (*SI Appendix*, Fig. S9). $T_{upper} = 200$ K is the temperature of the upper atmosphere and is assumed constant in our models. We conducted sensitivity tests with values of T_{upper} at 215 K and 170 K to cover warmer, Earth-like upper atmosphere temperatures (12) through to modern Venus's more intensely CO_2-cooled stratosphere (72) and found that the total number of successful runs is not sensitive to these variations in stratospheric temperature (*SI Appendix*, Fig. S10).

We calculate the energy-limited escape rate, given by the mass loss rate of H in a pure H atmosphere, using the following (69, 73):

$$\dot{M}_{H,ref} = \frac{\epsilon L_{XUV}(t) R^3}{4a^2 GM}, \quad [10]$$

$\epsilon = 0.15$ (69) is an efficiency factor, $L_{XUV}(t)$ is stellar XUV flux at time t, R is planet radius, a is Venus's semimajor axis, G is the gravitational constant, and M is the mass of Venus. To find $L_{XUV}(t)$, we use the following expression for solar XUV evolution, valid for solar age >0.1 Gyr (35, 73):

$$L_{XUV} = L_x (t/t_x)^{-\beta}, \quad [11]$$

where $t_x = 0.1$ Gyr, $\beta = 1.24$, and $L_x = 1.6 \times 10^{23}$ J s^{-1} is an upper bound on the Sun's early XUV flux.

For present-day Venus, the diffusion limit gives an H loss rate of order 10^{25} s^{-1}, depending on the mixing ratios of H and O in the resulting atmosphere, which is comparable to calculated modern H escape rates (74). We set $T_{upper} = 200$ K, consistent with a CO_2 dominated atmosphere (15, 75).

High-flux H escape can drag O along with it ref. 23 (*SI Appendix, Oxygen Loss Model*). This process is active during the first few million years of our models with habitable eras beginning at 4.0 Ga but is negligible relative to O loss through nonthermal escape and oxidation of lava flows and magma.

Escape of heavy species. For most of Venus's history, O loss to space has been via nonthermal escape processes. These depend on the XUV flux from the Sun and the properties of the solar wind (15, 21). We use existing studies' (21) calculations of maximum loss of O_2 from Venus's atmosphere as a function of time. As O_2 is a minor constituent of the atmosphere relative to CO_2, we assume that O_2 loss from the upper atmosphere is limited by diffusion through the background atmosphere similar to Eq. **8**:

$$m_{atm} = X_{CO_2} m_{CO_2} + X_{H_2O} m_{H_2O} + X_{CO} m_{CO} + X_{CH_4} m_{CH_4} + X_{CO} m_{CO} + X_{H_2} m_{H_2}.$$

In this case, we apply a binary diffusion coefficient (b) relevant to the diffusion of O_2 through a mixture of CO_2 and CO (following the same approach as for diffusion of H through the upper atmosphere, Eq. **9**) (71) as these are the dominant constituent of the atmosphere in the majority of our models. As for H escape, we find the nonthermal escape rate and calculate the diffusion limit for O and apply the smallest of the two to O escape in our models. Following other models of the long-term evolution of Venus's atmosphere, we neglect nonthermal losses of CO_2 (15, 76).

C. Degassing. For each model run, we set a melt H_2O and CO_2 concentration (c_{H_2O} and c_{CO_2}, respectively, Table 1), based on the range observed in terrestrial Mid Ocean Ridge Basalts (MORB) (77–80), which have similar bulk compositions to Venus basalts (81). We also set an oxidation state of the erupting melt between the fayalite–magnetite–quartz buffer ($logfO_2$ = FMQ ± 0) and $logfO_2$ = FMQ−4. We use VolcGasses (47) to find H_2O and CO_2 solubility in basaltic melt (s_{H_2O} and s_{CO_2}, respectively) and calculate the speciation of the exsolved H and C bearing gasses as a function of melt temperature and surface pressure. This degassing model assumes that bubbles and surrounding melt remain in thermodynamic equilibrium (47). We assume that melts reaching the surface degas at Venus's time-varying surface pressure and that all intrusive melts are emplaced at a shallow enough depth that all melt CO_2 can degas as CO_2, CO, or CH_4.

To calculate the degassing rate of H_2O per unit Venus surface area, we use:

$$\dot{M}_{H_2O,degas} = \dot{z}_{erupt} \rho_{melt} r_{H_2O} \left(c_{H_2O} - s_{H_2O}\right), \quad [12]$$

where $\dot{z}_{erupt}$ is the eruption rate (in m s^{-1}), ρ_{melt} is the density of the melt, and $r_{H_2O} = n_{H_2O}/(n_{H_2O} + n_{H_2})$ is the molar fraction of H_2O in the melt exsolved as H_2O. When $s_{H_2O} \geq c_{H_2O}$, $\dot{M}_{H_2O,degas} = 0$.

CO_2 solubilities in basaltic melt are much lower than our prescribed melt CO_2 concentrations at all pressures, so to calculate the degassing rate of CO_2 per unit Venus surface area, we use

$$\dot{M}_{CO_2,degas} = \dot{z}_{erupt} \rho_{melt} r_{CO_2} c_{CO_2}, \quad [13]$$

where $r_{CO_2} = n_{CO_2}/(n_{CO} + n_{CH_4}) + n_{CO_2}$ is the molar fraction of CO_2 in the melt exsolved as CO_2. We also calculate H_2, CO, and CH_4 degassing into the atmosphere at each time step using the same approach but substituting in r_{H2}, r_{CO}, and r_{CH4} as appropriate. After degassing, these species are oxidized by atmospheric O_2 (if present) to form H_2O and CO_2. If there are fewer moles of atmospheric O_2 in the atmosphere than would be needed to fully oxidize CO and CH_4, we assume that all the CO and CH_4 remaining after the O_2 are consumed stay in the atmosphere. This approach maximizes the likelihood of a model run matching both the modern O_2 and CO constraints on Venus's atmosphere because it both maximizes O_2 loss through this sink as well as maximizing oxidation of CO and CH_4 to CO_2.

The column mass of CO_2 in the atmosphere at the end of the habitable era is varied between 0% and 90% of Venus's present atmospheric CO_2. This accounts for any CO_2 either present in the atmosphere during the habitable era or added at the end of the habitable era through thermal decomposition of habitable era carbonates. We do not consider the 100% case because without volcanism, the sole O_2 sink on Venus is nonthermal escape, which has been quantified in existing studies (21). The remaining CO_2 is volcanically outgassed after the habitable era. The outgassing rate depends on initial conditions, model start time (end of the habitable era) and prescribed c_{CO_2}. We start each run by calculating z_{tot}, i.e., the total thickness of a global layer of lava needed to degas sufficient C species for Venus's modern atmosphere to have 90 bar CO_2:

$$z_{tot} = \frac{f_{volc}}{c_{CO_2} \rho_{melt}} M_{CO_2,f}. \quad [14]$$

The evolution of Venus's eruption rate is unknown, but the present-day eruption rate has been estimated at $\dot{z}_V = 0.1 - 0.2$ km^3 y^{-1} (82), and the total CO_2 concentration-dependent erupted thickness (z_{tot}) is set by the need to outgas enough C-bearing atmospheric species for Venus's modern atmosphere to have 90 bar of CO_2 minus any CO_2 present in the atmosphere at the model start time. Although models of Venus's crustal production based on different possible tectonic regimes exist (42, 83), the exact crustal production history is not known. The crater retention age of Venus's surface is young, suggesting that the planet has been resurfaced geologically recently (51, 52). However, the mechanism for resurfacing is debated. One hypothesis is a catastrophic resurfacing event 0.3 to 1 Gyr ago (53), for example, by episodic subduction with complete renewal of Venus's lithosphere every few hundred million years (42, 84), but an alternative is equilibrium resurfacing by continuous volcanism (54), which is also supported by evidence for ongoing volcanism (85). In our model, we use a highly simplified crustal production history for Venus that assumes continuous volcanism decreasing exponentially over time throughout Venus's history. This is similar to the pattern of melt production for full parameterized convection models of Venus (12). The total erupted volume is set by average melt CO_2 concentration and the proportion of CO_2 in Venus's atmosphere that is sourced from post-habitable era volcanism. We parameterize the eruption rate as an exponential (*SI Appendix*, Fig. S2):

$$\dot{z}_{erupt} = a \exp(-bt), \quad [15]$$

Downloaded from https://www.pnas.org by UNIVERSITY OF CHICAGO THE JOHN CRERAR LIBRARY on March 8, 2023 from IP address 128.135.55.25.

where t is time since the end of the habitable period, b, is the e-folding timescale of volcanism in Gyr, and a is a constant:

$$a = \frac{(\dot{z}_V / f_{ext}) + b\, z_{tot}}{1 - e^{-b\, t_{er}}}, \quad [16]$$

where $\dot{z}_V$ is the present-day crustal production rate, f_{ext} is the extrusive volcanism fraction, and t_{er} is either the end of the habitable era in model time (i.e., $4.5 - t_{start}$) or the model time at which the surface temperature drops below the basalt solidus in runs that begin with an RGH. We assume a modern crustal production rate of 0.1 $km^3\ y^{-1}$ (82, 86, 87). We vary f_{ext} from 0.1 to 1 because some of Venus's volcanism must be extrusive to account for the young crater retention age of Venus's surface, and extending to $f_{ext} = 1$ captures both Earth-like extrusive:intrusive volcanism ratios at $f_{ext} = 0.3$ and 0.5 (88) and extreme heat-pipe tectonics at $f_{ext} = 1$ (89). All times are in Gyr. b and $\dot{z}_V$ are the most uncertain parameters in this equation as Venus's crustal production history and present extrusive volcanism fraction are poorly constrained.

D. Oxidation of Basalt. O_2 left behind by H escape from the atmosphere may be removed by oxidation of basalt (24):

$$2FeO + 0.5O_2 \rightarrow Fe_2O_3. \quad [17]$$

The FeO concentrations at the Venera 13 and 14 landing sites are 9.3 ± 2.2 wt% and 8.8 ± 1.8 wt%, respectively (59), with bulk compositions at the Venera 14 and Vega 2 landing sites similar to terrestrial Mid Ocean Ridge Basalts (MORB) (81). The typical FeO concentration in MOR basalts on the Earth is between 7 and 12 wt% (90). We assume that erupted lava on Venus contains an average of 10 wt% FeO, such that 0.1 kg of FeO are emplaced on Venus' surface for each 1 kg of lava. We follow ref. 21 and assume that 1% of lava erupted on Venus is oxidized (*SI Appendix, Oxygen Loss Model*), corresponding to the top 1 cm of a 1-m thick flow. We also assume that lava cannot continue to be oxidized past the timestep when it is produced because it will be buried by subsequent lava flows and diffusion in solid basalt is too slow for buried basalt to remain in contact with atmospheric O_2. The mass of O_2 removed from the atmosphere in a given timestep ($\dot{M}_{O_2,ox}$) is

$$\dot{M}_{O2,ox} = M_{O2,atm} - 0.01 m_{O2} \frac{0.25 \rho c_{FeO} f_{ex} z_{erupt}(t)}{m_{FeO}}, \quad [18]$$

where m_{O2} and m_{FeO} are the molecular masses of O_2 and FeO, respectively, and c_{FeO} is the typical concentration of FeO in basalt in wt%. The factor of 0.25 accounts for the stoichiometry of Eq. **17**. $M_{O2,atm}$ is not allowed to fall below 0.

Volcanism on Venus may not always have been dominated by lava flows. Basaltic eruptions on Earth can be explosive, producing large volumes of ash and scoria (91). We include a procedure for calculating whether or not explosive volcanism is occurring at a given timestep and for calculating the corresponding O_2 sink of the ash and scoria produced (*SI Appendix, Oxygen Loss Model*). When explosive volcanism is active, we assume that all FeO in basaltic material can be oxidized based on the short oxidation timescales of sub-cm fragments in experiments even under modern Venus conditions (92).

E. Radiogenic Ar Degassing Model. Following previous work (27, 28), we model the evolution of Venus's mantle, crust, and atmosphere ^{40}K and ^{40}Ar inventories forward in time starting from the end of a hypothetical habitable era (*SI Appendix, Radiogenic Ar Degassing Model for details*). Our models begin with mantle ^{40}K concentrations set by the decay of ^{40}K from Venus formation to the end of the habitable era and with some fraction of the resulting radiogenic ^{40}Ar (f_{pre} ranging from 0 to 1) in the atmosphere.

^{40}Ar degassing occurs as a result of crustal production. New crust is produced by melting of the mantle at the crustal production rate set by the parameters t_{end}, f_{volc}, f_{ext}, and c_{CO_2} in our Oxygen Loss Model. We also consider an additional four parameters: crustal thickness, average melt fraction, and Venus's primordial mantle U concentration and K/U ratio (*SI Appendix*, Table S2) (27, 28). During partial melting, ^{40}K and ^{40}Ar preferentially partition into the melt, enriching the melt in these species. We assume that ^{40}Ar partitioned into the melt is released instantaneously into the atmosphere (28) and the ^{40}K enters the crust. The ^{40}K in the newly erupted crust decays over time to produce more ^{40}Ar that we assume diffuses rapidly to the atmosphere (28). To calculate this ^{40}Ar release at each timestep, we find the ^{40}K decay integrated across the entire depth of the crust, which we assume has a fixed thickness. We track the ^{40}K concentration throughout the crust at depth intervals of 1 m and consider cases both with and without recycling of ^{40}K back into the mantle (*SI Appendix*, Fig. S5).

Example ^{40}Ar degassing runs for a range of crustal production histories are shown in *SI Appendix*, Fig. S3. Model runs with final atmospheric ^{40}Ar inventories that match Venus's modern atmospheric composition are marked as successful. We then find the proportion of successful Ar degassing runs overall and for each unique combination of t_{end}, f_{volc}, f_{ext}, and c_{CO_2}. We multiply these by our oxygen loss model success rates to find the overall proportion of runs that can successfully match Venus's modern atmospheric composition (Fig. 5).

F. Water Recycling During the Habitable Era. To determine the conditions under which hydrated crust can be recycled into the mantle during a hypothetical habitable era, we calculate 1-D steady state geotherms for lithosphere of a fixed thickness z_{lith} and with a fixed downward advection velocity v equal to the crustal production rate. We assume a heat pipe-style regime where new crust is produced through extrusive volcanism, leading to burial of older crust, and the eventual recycling of material from the base of the lithosphere into the underlying convecting mantle (42). The resulting geotherm (38, 39) is compared to phase boundaries for eclogite formation (40) and serpentinite dehydration (41). If eclogite formation is enabled first, then hydrated crust is recycled into the mantle (*SI Appendix, Habitable Era Water Recycling Model* for details).

Data, Materials, and Software Availability. All of the code for this paper, including instructions to reproduce all figures, can be found on GitHub at https://github.com/aowarren/Venus_O2. Data from completed model runs can be obtained via Zenodo at https://zenodo.org/record/7416204#.Y5UVEXbMK3A.

ACKNOWLEDGMENTS. This project made use of University of Chicago Research Computing Center resources. Grants: NASA NNH19ZDA001N-FINESST (F.I.A.O. Warren).

1. J. O'Callaghan, How three missions to Venus could solve the planet's biggest mysteries. *Nature* **594**, 486–487 (2021).
2. M. Y. Zolotov, B. Fegley Jr, K. Lodders, Hydrous silicates and water on Venus. *Icarus* **130**, 475–494 (1997).
3. K. Hamano, Y. Abe, H. Genda, Emergence of two types of terrestrial planet on solidification of magma ocean. *Nature* **497**, 607–610 (2013).
4. C. Gillmann, E. Chassefière, P. Lognonné, A consistent picture of early hydrodynamic escape of Venus atmosphere explaining present Ne and Ar isotopic ratios and low oxygen atmospheric content. *Earth Planet. Sci. Lett.* **286**, 503–513 (2009).
5. M. Turbet *et al.*, Day-night cloud asymmetry prevents early oceans on Venus but not on Earth. *Nature* **598**, 276–280 (2021).
6. J. B. Pollack, A nongrey calculation of the runaway greenhouse: Implications for Venus' past and present. *Icarus* **14**, 295–306 (1971).
7. J. Yang, G. Boué, D. C. Fabrycky, D. S. Abbot, Strong dependence of the inner edge of the habitable zone on planetary rotation rate. *Astrophys. J.* **787**, L2 (2014).
8. M. J. Way, A. D. Del Genio, Venusian habitable climate scenarios: Modeling Venus through time and applications to slowly rotating Venus-like exoplanets. *J. Geophys. Res.: Planets* **125**, e2019JE006276 (2020).
9. M. J. Way *et al.*, Was Venus the first habitable world of our solar system? *Geophys. Res. Lett.* **43**, 8376–8383 (2016).
10. J. F. Kasting, Runaway and moist greenhouse atmospheres and the evolution of Earth and Venus. *Icarus* **74**, 472–494 (1988).
11. A. Salvador *et al.*, The relative influence of H_2O and CO_2 on the primitive surface conditions and evolution of rocky planets. *J. Geophys. Res.: Planets* **122**, 1458–1486 (2017).
12. J. Krissansen-Totton, J. J. Fortney, F. Nimmo, Was Venus ever habitable? Constraints from a coupled interior-atmosphere-redox evolution model. *Planet. Sci. J.* **2**, 216 (2021).
13. C. De Bergh *et al.*, Deuterium on Venus: Observations from earth. *Science* **251**, 547–549 (1991).
14. T. M. Donahue, J. H. Hoffman, R. R. Hodges, A. J. Watson, Venus was wet: A measurement of the ratio of deuterium to hydrogen. *Science* **216**, 630–633 (1982).
15. Y. Kulikov *et al.*, Atmospheric and water loss from early Venus. *Planet. Space Sci.* **54**, 1425–1444 (2006).
16. T. M. Donahue, New analysis of hydrogen and deuterium escape from Venus. *Icarus* **141**, 226–235 (1999).
17. D. H. Grinspoon, Implications of the high D/H ratio for the sources of water in Venus' atmosphere. *Nature* **363**, 428–431 (1993).

Downloaded from https://www.pnas.org by UNIVERSITY OF CHICAGO THE JOHN CRERAR LIBRARY on March 8, 2023 from IP address 128.135.55.25.

18. F. Selsis *et al*., Habitable planets around the star Gliese 581? *Astron. Astrophys.* **476**, 1373–1387 (2007).
19. J. Horner, O. Mousis, J. M. Petit, B. Jones, Differences between the impact regimes of the terrestrial planets: Implications for primordial d:H ratios. *Planet. Space Sci.* **57**, 1338–1345 (2009).
20. K. Pahlevan, L. Schaefer, M. M. Hirschmann, Hydrogen isotopic evidence for early oxidation of silicate earth. *Earth Planet. Sci. Lett.* **526**, 115770 (2019).
21. C. Gillmann *et al*., Dry late accretion inferred from Venus's coupled atmosphere and internal evolution. *Nat. Geosci.* **13**, 265–269 (2020).
22. A. P. Ingersoll, The runaway greenhouse: A history of water on Venus. *J. Atmos. Sci.* **26**, 1191–1198 (1969).
23. F. Tian, History of water loss and atmospheric O_2 buildup on rocky exoplanets near M dwarfs. *Earth Planet. Sci. Lett.* **432**, 126–132 (2015).
24. A. W. Heard, E. S. Kite, A probabilistic case for a large missing carbon sink on Mars after 3.5 billion years ago. *Earth Planet. Sci. Lett.* **531**, 116001 (2020).
25. V. Moroz, The atmosphere of Venus. *Space Sci. Rev.* **29**, 3–127 (1981).
26. N. M. Johnson, M. R. R. de Oliveira, Venus atmospheric composition in situ data: A compilation. *Earth Space Sci.* **6**, 1299–1318 (2019).
27. J. G. O'Rourke, J. Korenaga, Thermal evolution of Venus with argon degassing. *Icarus* **260**, 128–140 (2015).
28. W. M. Kaula, Constraints on Venus evolution from radiogenic argon. *Icarus* **139**, 32–39 (1999).
29. E. Chassefière, Hydrodynamic escape of oxygen from primitive atmospheres: Applications to the cases of Venus and Mars. *Icarus* **124**, 537–552 (1996).
30. C. Gillmann, E. Chassefière, P. Lognonné, A consistent picture of early hydrodynamic escape of Venus atmosphere explaining present Ne and Ar isotopic ratios and low oxygen atmospheric content. *Earth Planet. Sci. Lett.* **286**, 503–513 (2009).
31. J. Deng, Z. Du, B. B. Karki, D. B. Ghosh, K. K. Lee, A magma ocean origin to divergent redox evolutions of rocky planetary bodies and early atmospheres. *Nat. Commun.* **11**, 1–7 (2020).
32. E. Cottrell, K. A. Kelley, The oxidation state of Fe in MORB glasses and the oxygen fugacity of the upper mantle. *Earth Planet. Sci. Lett.* **305**, 270–282 (2011).
33. K. Zahnle *et al*., Emergence of a habitable planet. *Space Sci. Rev.* **129**, 35–78 (2007).
34. M. Turbet, D. Ehrenreich, C. Lovis, E. Bolmont, T. Fauchez, The runaway greenhouse radius inflation effect - An observational diagnostic to probe water on Earth-sized planets and test the habitable zone concept. *Astron. Astrophys.* **628**, A12 (2019).
35. I. Ribas, E. F. Guinan, M. Gudel, M. Audard, Evolution of the solar activity over time and effects on planetary atmospheres I. High-energy irradiances (1–1700 Å). *Astrophys. J.* **622**, 680–694 (2005).
36. B. J. Foley, A. J. Smye, Carbon cycling and habitability of Earth-sized stagnant lid planets. *Astrobiology* **18**, 873–896 (2018).
37. A. Morschhauser, M. Grott, D. Breuer, Crustal recycling, mantle dehydration, and the thermal evolution of Mars. *Icarus* **212**, 541–558 (2011).
38. T. C. O'Reilly, G. F. Davies, Magma transport of heat on Io: A mechanism allowing a thick lithosphere. *Geophys. Res. Lett.* **8**, 313–316 (1981).
39. D. G. Kankanamge, W. B. Moore, A parameterization for volcanic heat flux in heat pipe planets. *J. Geophys. Res.: Planets* **124**, 114–127 (2019).
40. K. Bucher, M. Frey, "Metamorphism of mafic rocks" in *Petrogenesis of Metamorphic Rocks* (Springer, 2002), pp. 279–324.
41. B. R. Hacker, G. A. Abers, S. M. Peacock, Subduction factory 1. Theoretical mineralogy, densities, seismic wave speeds, and H_2O contents. *J. Geophys. Res.: Solid Earth* **108** (2003).
42. M. Armann, P. J. Tackley, Simulating the thermochemical magmatic and tectonic evolution of Venus's mantle and lithosphere: Two-dimensional models. *J. Geophys. Res.: Planets* **117** (2012).
43. D. Hasterok, J. Webb, On the radiogenic heat production of igneous rocks. *Geosci. Front.* **8**, 919–940 (2017).
44. P. B. James, M. T. Zuber, R. J. Phillips, Crustal thickness and support of topography on Venus. *J. Geophys. Res.: Planets* **118**, 859–875 (2013).
45. L. Schaefer, D. Sasselov, The persistence of oceans on Earth-like planets: Insights from the deep-water cycle. *Astrophys. J.* **801**, 40 (2015).
46. S. E. Smrekar, A. Davaille, C. Sotin, Venus interior structure and dynamics. *Space Sci. Rev.* **214**, 1–34 (2018).
47. N. Wogan, J. Krissansen-Totton, D. C. Catling, Abundant atmospheric methane from volcanism on terrestrial planets is unlikely and strengthens the case for methane as a biosignature. *Planet. Sci. J.* **1**, 58 (2020).
48. M. A. Bullock, D. H. Grinspoon, The recent evolution of climate on Venus. *Icarus* **150**, 19–37 (2001).
49. D. V. Titov *et al*., *Radiation in the Atmosphere of Venus* (American Geophysical Union, 2007), pp. 121–138.
50. D. V. Titov, G. Piccioni, P. Drossart, W. J. Markiewicz, *Radiative Energy Balance in the Venus Atmosphere*, L. Bengtsson et al., Eds. (Springer, New York, 2013), pp. 23–53.
51. R. J. Phillips *et al*., Impact craters and Venus resurfacing history. *J. Geophys. Res.: Planets* **97**, 15923–15948 (1992).
52. W. F. Bottke *et al*., "On asteroid impacts, crater scaling laws, and a proposed younger surface age for Venus" in *Lunar and Planetary Science Conference, Lunar and Planetary Science Conference* (2016), p. 2036.
53. R. G. Strom, G. G. Schaber, D. D. Dawson, The global resurfacing of Venus. *J. Geophys. Res.: Planets* **99**, 10899–10926 (1994).
54. E. Bjonnes, V. L. Hansen, B. James, J. B. Swenson, Equilibrium resurfacing of Venus: Results from new Monte Carlo modeling and implications for Venus surface histories. *Icarus* **217**, 451–461 (2012).
55. J. G. O'Rourke, Venus: A thick basal magma ocean may exist today. *Geophys. Res. Lett.* **47**, e2019GL086126 (2020).
56. I. H. Campbell, S. R. Taylor, No water, no granites - No oceans, no continents. *Geophys. Res. Lett.* **10**, 1061–1064 (1983).
57. J. G. Shellnutt, Petrological modeling of basaltic rocks from Venus: A case for the presence of silicic rocks. *J. Geophys. Res.: Planets* **118**, 1350–1364 (2013).
58. M. D. Dyar, J. Helbert, A. Maturilli, N. T. Müller, D. Kappel, Probing Venus surface iron contents with six-band visible near-infrared spectroscopy from orbit. *Geophys. Res. Lett.* **47**, e2020GL090497 (2020).
59. Yu. A. Surkov, V. L. Barsukov, L. P. Moskalyeva, V. P. Kharyukova, A. L. Kemurdzhian, New data on the composition, structure, and properties of Venus rock obtained by Venera 13 and Venera 14. *J. Geophys. Res.: Solid Earth* **89**, B393–B402 (1984).
60. D. Höning, P. Baumeister, J. L. Grenfell, N. Tosi, M. J. Way, Early habitability and crustal decarbonation of a stagnant-lid venus. *J. Geophys. Res.: Planets* **126**, e2021JE006895 (2021).
61. D. Kerrick, J. Connolly, Metamorphic devolatilization of subducted marine sediments and the transport of volatiles into the Earth's mantle. *Nature* **411**, 293–296 (2001).
62. R. D. Wordsworth, R. T. Pierrehumbert, Water loss from terrestrial planets with CO_2-rich atmospheres. *Astrophys. J.* **778**, 154 (2013).
63. M. Turbet *et al*., Revised mass-radius relationships for water-rich rocky planets more irradiated than the runaway greenhouse limit. *Astron. Astrophys.* **638**, A41 (2020).
64. C. Lécuyer, L. Simon, F. Guyot, Comparison of carbon, nitrogen and water budgets on Venus and the Earth. *Earth Planet. Sci. Lett.* **181**, 33–40 (2000).
65. L. Schaefer, R. D. Wordsworth, Z. Berta-Thompson, D. Sasselov, Predictions of the atmospheric composition of GJ 1132b. *Astrophys. J.* **829**, 63 (2016).
66. P. M. Smith, P. D. Asimow, Adiabat_1ph: A new public front-end to the MELTS, pMELTS, and pHMELTS models. *Geochem. Geophys. Geosyst.* **6** (2005).
67. P. D. Asimow, M. S. Ghiorso, Algorithmic modifications extending MELTS to calculate subsolidus phase relations. *Am. Mineral.* **83**, 1127–1132 (1998).
68. M. S. Ghiorso, R. O. Sack, Chemical mass transfer in magmatic processes IV. A revised and internally consistent thermodynamic model for the interpolation and extrapolation of liquid-solid equilibria in magmatic systems at elevated temperatures and pressures. *Contrib. Mineral. Petrol.* **119**, 197–212 (1995).
69. F. Tian, Atmospheric escape from solar system terrestrial planets and exoplanets. *Ann. Rev. Earth Planet. Sci.* **43**, 459–476 (2015).
70. K. J. Zahnle, J. F. Kasting, Mass fractionation during transonic escape and implications for loss of water from Mars and Venus. *Icarus* **68**, 462–480 (1986).
71. T. R. Marrero, E. A. Mason, Gaseous diffusion coefficients. *J. Phys. Chem. Ref. Data* **1**, 3–118 (1972).
72. M. Pätzold *et al*., The structure of Venus' middle atmosphere and ionosphere. *Nature* **450**, 657–660 (2007).
73. K. J. Zahnle, D. C. Catling, The cosmic shoreline: The evidence that escape determines which planets have atmospheres, and what this may mean for proxima centauri B. *Astrophys. J.* **843**, 122 (2017).
74. H. Lammer *et al*., Loss of hydrogen and oxygen from the upper atmosphere of Venus. *Planet. Space Sci.* **54**, 1445–1456 (2006).
75. C. P. Johnstone, M. Güdel, H. Lammer, K. G. Kislyakova, Upper atmospheres of terrestrial planets: Carbon dioxide cooling and the Earth's thermospheric evolution. *Astron. Astrophys.* **617**, A107 (2018).
76. C. Gillmann, G. J. Golabek, P. J. Tackley, Effect of a single large impact on the coupled atmosphere-interior evolution of Venus. *Icarus* **268**, 295–312 (2016).
77. A. E. Saal, E. H. Hauri, C. H. Langmuir, M. R. Perfit, Vapour undersaturation in primitive mid-ocean-ridge basalt and the volatile content of Earth's upper mantle. *Nature* **419**, 451–455 (2002).
78. L. V. Danyushevsky, The effect of small amounts of H_2O on crystallisation of mid-ocean ridge and backarc basin magmas. *J. Volcanol. Geotherm. Res.* **110**, 265–280 (2001).
79. S. Soule *et al*., CO_2 variability in mid-ocean ridge basalts from syn-emplacement degassing: Constraints on eruption dynamics. *Earth Planet. Sci. Lett.* **327**, 39–49 (2012).
80. C. Helo, M. A. Longpré, N. Shimizu, D. A. Clague, J. Stix, Explosive eruptions at mid-ocean ridges driven by CO_2-rich magmas. *Nat. Geosci.* **4**, 260–263 (2011).
81. J. Kargel, G. Komatsu, V. Baker, R. Strom, The volcanology of Venera and VEGA landing sites and the geochemistry of Venus. *Icarus* **103**, 253–275 (1993).
82. A. Basilevsky, J. Head, G. Schaber, R. Strom, "The resurfacing history of Venus " in *Venus II*, R. P. S. W. Bougher, D. M. Hunten, Eds. (University of Arizona Press, Tuscon, 1997).
83. M. B. Weller, W. S. Kiefer, The physics of changing tectonic regimes: Implications for the temporal evolution of mantle convection and the thermal history of Venus. *J. Geophys. Res.: Planets* **125**, e2019JE005960 (2020).
84. D. L. Turcotte, An episodic hypothesis for Venusian tectonics. *J. Geophys. Res.: Planets* **98**, 17061–17068 (1993).
85. S. E. Smrekar *et al*., Recent hotspot volcanism on Venus from VIRTIS emissivity data. *Science* **328**, 605–608 (2010).
86. R. G. Strom, G. G. Schaber, D. D. Dawson, The global resurfacing of Venus. *J. Geophys. Res.: Planets* **99**, 10899–10926 (1994).
87. M. A. Ivanov, J. W. Head, The history of volcanism on Venus. *Planet. Space Sci.* **84**, 66–92 (2013).
88. S. M. White, J. A. Crisp, F. J. Spera, Long-term volumetric eruption rates and magma budgets. *Geochem. Geophys. Geosyst.* **7** (2006).
89. W. B. Moore, J. I. Simon, A. A. G. Webb, Heat-pipe planets. *Earth Planet. Sci. Lett.* **474**, 13–19 (2017).
90. C. H. Langmuir, E. M. Klein, T. Plank, *Petrological Systematics of Mid-Ocean Ridge Basalts: Constraints on Melt Generation Beneath Ocean Ridges in Mantle Flow and Melt Generation at Mid-Ocean Ridges* (American Geophysical Union, 2013), pp. 183–280.
91. B. Houghton, H. Gonnermann, Basaltic explosive volcanism: Constraints from deposits and models. *Geochemistry* **68**, 117–140 (2008).
92. G. Berger *et al*., Experimental exploration of volcanic rocks-atmosphere interaction under Venus surface conditions. *Icarus* **329**, 8–23 (2019).

Downloaded from https://www.pnas.org by UNIVERSITY OF CHICAGO THE JOHN CRERAR LIBRARY on March 8, 2023 from IP address 128.135.55.25.